A Model Predictive Control Approach for Virtual Coupling in Railways

Jesus Felez, *Senior Member, IEEE*, Yeojun Kim, and Francesco Borrelli, *Fellow, IEEE*

***Abstract*— This paper presents a novel approach in train control systems based on the concept called virtual coupling or train convoys. This approach follows the recent developments in the field of safe platooning of autonomous vehicles. We use a decentralized model predictive control (MPC) framework for each train participating in a convoy formation. Control designs for the leading and following trains are presented. An optimal control formulation for both controllers is used and its design relies on a numeric solution of a finite horizon optimal control problem. This paper compares the proposed method with alternative control strategies including the well-studied moving block train control concept. A study of a metro line has been chosen as a first analysis for this control approach. The simulation results for this kind of railway lines demonstrate better performance and the benefits of this new concept versus the moving block system. We show that the virtual coupling concept substantially reduces headway and distance between trains while guaranteeing safe separation between two consecutive trains at any instant.**

***Index Terms*— CBTC, ERTMS, moving block, MPC, train convoy, train control systems, virtual coupling.**

I. Introduction

RAIL transport demand continues to rise around the world. This increase can be satisfied by multiplying the number of railway lines or by increasing the capacity of the existing ones. The first solution involves the construction of new lines, but this solution is usually very expensive. The railway industry has focused its efforts on increasing the capacity of the lines, improving the current railway operation. For this reason, the main objective of the modern traffic control and signaling railway systems based on the moving block concept is to increase the capacity by reducing the time interval or headway between trains, always guaranteeing traffic safety. Examples of these systems are CBTC [1], mainly used in urban railway lines and APMs, and ERTMS L3 [2] for main lines.

The study of these train control systems is widely discussed in the bibliography, covering not only topics related with line capacity and design [3]–[8], but also with the implications of physical implementations [9], [10].

Manuscript received May 30, 2018; revised April 1, 2019; accepted April 30, 2019. Date of publication May 20, 2019; date of current version June 26, 2019. The Associate Editor for this paper was S. E. Li. *(Corresponding author: Jesus Felez.)*

J. Felez is with the Department of Mechanical Engineering, Universidad Politecnica de Madrid, 28016 Madrid, Spain (e-mail: jesus.felez@upm.es).

Y. Kim is with the MPC Lab, University of California at Berkeley, Berkeley, CA 94720-1740 USA (e-mail: yk4938@berkeley.edu).

F. Borrelli is with the Department of Mechanical Engineering, University of California at Berkeley, Berkeley, CA 94720-1740 USA (e-mail: fborrelli@berkeley.edu).

Digital Object Identifier 10.1109/TITS.2019.2914910

The moving block system is based on the fact that the trains continuously calculate and communicate their exact position and speed to the wayside equipment distributed along the line, allowing the calculation of the area potentially occupied by the train on the track, and making the trains automatically and continuously adjust their speed while maintaining the safety and comfort requirements. The moving block system makes the assumption that consecutive trains on the same track must be separated by a sufficient margin to ensure that every train is capable of braking and stopping before reaching the last known position of the train in front at any time. However, this conservative behavior causes a large gap between trains. In reality, depending on the braking rates of the two consecutive trains, the safety margin between two consecutive trains can be reduced. Moreover, a communication link between the trains can also help further minimizing this margin.

Building upon this concept, a more advanced approach in train control systems called Train Convoy or Virtual Coupling is considered, similar to the mode of on road operations, where vehicles circulate keeping a safe distance with the preceding vehicle and the driver reacts to the brake lights of the vehicle in front. This safe distance is much lower than the braking distance needed for a full stop. This idea is one of the fundamentals of autonomous driven vehicles and vehicle platooning. This concept in railways is known as train Convoy or Virtual Coupling.

Virtual Coupling is strictly related to cooperative driving. Trains are virtually-coupled via train-to-train communication, sharing information with neighbors and receiving the reference signals coming from the infrastructure. On the basis of this information received from trains within the convoy, the on-board system is responsible for the safe tracking of speed profiles, while respecting the inter-train spacing policy, allowing the follower to pursue the leader train in a safe way and guaranteeing good transient dynamics.

The virtual coupling concept presents several advantages. First, it increases the line capacity. In addition, in virtual coupling, trains can be coupled and decoupled dynamically, according to the service needs and respecting the safety requirements. This is a key point in the approaching of very long trains to short platforms, allowing the convoy to be uncoupled in shorter trains when entering the station.

An initial idea of virtual train operation appeared in [11] and [12], where the authors present an operating concept and its design for railways, in which the wagons are no longer physically coupled, and every wagon has got its own propulsion and computer system. The concept also does not

use block systems and the vehicles drive in a minimal distance as short as mechanically coupled cars. The paper describes the methods to design and develop the concept, however it does not provide many implementation details. In a similar way [13] and [14] discussed the basic concept of virtually coupled train formations, the methodological approach and results presenting the basic functionality of the concept.

The paper in [15] presents the idea of an operational and safety concept for railway operation with a platoon of trains which are linked by a wireless informational interconnection instead of a conventional mechanical connection. And [16] introduces the development of autonomous railway vehicles which can dynamically group to convoys without mechanical coupling, presenting the convoy communication with respect to joining and leaving a convoy as well as the convoy control strategy.

In summary, the state of the art shows that the concept of virtual coupling has been extensively studied. However, its approach, more oriented to the freight transport, and the existing limitations of the technology in the past, has not allowed to develop its real potential.

A new impulse to this concept arises when the European research initiative Shift2Rail [17], [18] appeared, mainly motivated by the need of increasing the flexibility, interoperability and capacity of the passenger lines, and by the achievements in the communications technology field. Recent publications try to analyze the problem of this concept and propose future lines of actuation. In this way, IRSE in their technical document [19] shows an analysis of the virtual coupling concept, making a first assessment about if it is technically feasible, if it is safe, and if it will deliver real benefits. Their conclusion is that virtual coupling is an interesting idea that must be explored.

Reference [20] presents the technologies required for virtual coupling implementation which will be developed within the Shift2Rail initiative. Its conclusion states that nowadays emerging technologies from the telecommunication, sensors, and computing worlds make feasible to introduce such concept in railways, while the leverage effect coming from the car industry and their large scale sales will smooth the acceptance of the concept and moderate the costs. Virtual coupling also introduces some critical issues related to potential hazards as well as strict tolerated latency requirements associated with the channels used for the train-to-trackside and the train-to-train communications.

From the state of the art, it is clear that the concept of virtual coupling has been analyzed, and the elements that would be technically necessary have been identified. But, to date, no theoretical or simulation studies have been carried out that analyze and design the more suitable control system for the virtual coupling concept. This work tries to cover this, carrying out a study on the control system to be used for virtual coupling.

The goal of this paper is to propose an innovative solution in the field of railways for train virtual coupling following the ideas coming from the developments in the platooning of autonomous vehicles, based on the Model Predictive Control (MPC) framework. This technique has been successfully used in many industrial applications, like thermal energy control [21], collision avoidance [22], vehicle stability [23], and energy management [24].

Model predictive control (MPC) is a control algorithm that relies on the iterative solution of an optimal control problem based on the predicted state to compute a control input at each sampling. The prediction of the state is based on a system model. The popularity of MPC stems from the fact that the resulting operating strategy respects all the system and problem constraints. For this reason, MPC is adopted for our control design.

On the other hand, the platooning of autonomous vehicles has received considerable attention in recent years, due to its potential to significantly benefit road transportation, including improving traffic efficiency, enhancing road safety, and reducing fuel consumption [25]–[29].

This paper presents a first study to explore the feasibility and the hypothetical advantages of virtual coupling in railways through simulation. The objective of the simulations is to show differences between the proposed and existing control strategies, from an operational point of view, i.e. analyzing trip times, time delays and distance between trains, comparing the new virtual coupling control system versus the previous moving block concept.

First, we have developed a simple scenario to check and evaluate several basic aspects. This scenario is used to evaluate the influence of the horizon prediction length, the system performance when we use a convoy with multiple trains, and the differences between the different prediction strategies.

After that, a study of a metro line has been chosen to analyze this control in a real circulation environment. The data considered in the simulations correspond to real data belonging to Line 1 of Metro of Ho Chi Minh in Vietnam, obtained from [30]. The simulations cover the whole line with fourteen stations and a train convoy formed by two trains. The reason is because the study is limited to a metro line and the length of the platform and the length of the trains only allow two trains to be at the same time in a given station. The second assumption is that this work only considers a single line and no crossing between different lines have been analyzed, so the results of this paper are restricted to this kind of railway lines.

There are two possible control architectures for virtual coupling. The first one is a control architecture for a cooperative control of trains by using a centralized control, called centralized virtual coupling. In this framework, trains cooperate in order to optimize the overall convoy strategy. The second control architecture is a decentralized control, called decentralized virtual coupling. In this case, each train optimizes its own strategy given the estimation of the preceding vehicle trajectory.

The first control architecture, used for the centralized control of trains, implies that a complex centralized control system acts simultaneously in the whole train convoy and superimposed on the signaling system. In a real implementation it is supposed to have a high implementation cost. Not only needs the necessary onboard equipment including additional sensors like radars or lidars, but also a communication link of each train with the Centralized Traffic Control (CTC) and the implementation of the control laws in the CTC. Solving a

single optimization for the whole system with multiple trains can impose a high computational burden, which scales poorly with the number of trains.

The decentralized virtual coupling control architecture is simpler to implement. The leader follows the signaling system implemented in the line (CBTC for example) and the follower makes its decisions based only on the information provided by the preceding train. The trains only need the additional onboard sensors to control their position with respect to the preceding train, receiving distance and speed information and brake demand data from the preceding train; i.e. each train has its own onboard controller which only uses data available from its V2V communication and other onboard sensors. From a computational point of view, it is simpler because computational burden is distributed to each individual train.

In any case, the follower falls back to Level 3 if loses connection with the leader.

The approach used in this paper is based on the second scheme, studying decentralized and safe controllers for each train participating in a convoy formation. A more complex centralized controller for cooperative virtual coupling will be the object of future research.

The contribution of this paper is a novel approach in train control systems that, using the concept of virtual coupling and MPC, develops a control system that substantially reduces distance between trains while guaranteeing safe separation between two consecutive trains at any instant, as will be demonstrated through the simulation results.

The remainder of this paper is organized as follows. Section II defines the problem under study and the dynamic model considered. Section III formulates the nonlinear MPC developed for virtual coupling including the variables to be optimized, the cost function and the different constraints that have been considered. This section also includes the explanation of the different control strategies that have been analyzed. Section IV presents the different test, simulations and results. Finally, Section V includes the conclusions of this work.

II. Dynamic Model

The model used in this paper is based on the longitudinal train dynamics (LTD), considering the train as a point mass with 1 d.o.f., the driving/braking system, the rolling and bearing resistances, the air input, the aerodynamic drag, and the grade and curving resistances. Reference [32] presents a complete overview of LTD. The model has been developed following the guidelines shown in [31] and [32]. The dynamic equation are:

$$\dot{s} = v \tag{1a}$$

$$M\dot{v} = -A - Bv - T_f C v^2 - F_e + u \tag{1b}$$

$$\dot{F} = (u - F)/\tau \tag{1c}$$

where $v(m/s)$ and $s(m)$ denote the train velocity and position, respectively; $u(N)$ is the controlled driving or braking force; $F(N)$ is the integrated driving/braking force; $F_e(N)$ is the external force due to the track; τ is the inertial lag of longitudinal dynamics; $M(kg)$ is the mass; $A(N)$ is a term that includes the rolling resistance plus the bearing resistance; $B(Ns/m)$ is a coefficient related with the air input; $C(Ns^2/m^2)$ is the aerodynamic coefficient and T_f is the tunnel factor.

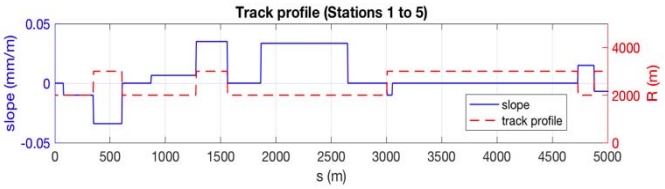

Fig. 1. Slope and curve radius considered in the simulations for the line. Detail including only the first five stations.

In the model, *M, A, B* and *C* are parameters that depend on the train characteristics.

The starting resistance associated with the characteristics of dry friction is included as an additional value in A. This implies a higher friction coefficient at a lower speed and A depends on v. In our case, the starting resistance is neglected when speed is higher than 3m/s.

The external force F_e considers two different components, F_g and F_R, being:

$$F_e = F_g + F_R \tag{2a}$$

$$F_g = -Mg \times slope \tag{2b}$$

$$F_R = -M \times 6 \times 10^6/R \tag{2c}$$

where $F_g(N)$ is the gravity force component due to track grade, $slope(mm/m)$ is the track grade, $g(m/s^2)$ is the gravity acceleration, $F_R(N)$ is the curving resistance and $R(m)$ is the radius of the curve.

We assume the values of *slope* and R are known at each time and are dependent on the line profile and the train location on the line, i.e. the train position s. Fig. 1 shows the value of slope and R used in the simulation scenario of this paper obtained from [30]. In this figure only a reduced number of stations (1 to 5) have been included in order to highlight line information details.

The controlled driving or braking force u is obtained as:

$$u = F_{dr} - F_{br} \tag{3}$$

where F_{dr} is the driving effort or the dynamic braking force (for service braking) and F_{br} is the braking resistance due to pneumatic braking.

The force u is subject to the following constraints:

$$u \in [-Ma_{br}, Ma_{dr}] \tag{4a}$$

$$u \cdot v \in [-P_{br}, P_{dr}] \tag{4b}$$

$$\dot{u}/M \in [-j_{max}, j_{max}] \tag{4c}$$

where P_{dr} is the driving power; P_{br} is the braking power; a_{dr} is the maximum driving acceleration; a_{br} is the maximum braking deceleration and j_{max} the maximum jerk. Note that a_{dr} and a_{br} are directly related with the adhesion limitation μ_{dr} and μ_{br} which determine the maximum available traction/braking force. In this model we consider a constant adhesion limitation, i.e.

$$a_{br} = \mu_{br} g \tag{5a}$$

$$a_{dr} = \mu_{dr} g \tag{5b}$$

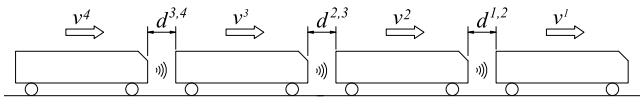

Fig. 2. General train convoy.

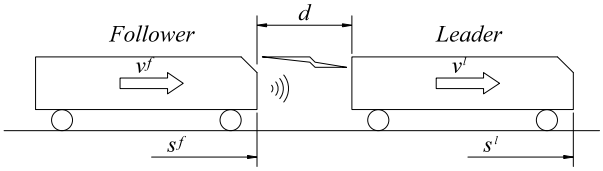

Fig. 3. Trains considered in the simulation.

The equations (1) can be written in a compact way as (6a). To apply model predictive control, we discretize the dynamics shown in (6a) obtaining the state update equations in (6b).

$$\dot{x} = f_t(x, u) \tag{6a}$$

$$x(k+1) = x(k) + \Delta t \cdot f_t(x(k), u(k)) \tag{6b}$$

being $x = \left(s \; v \; F\right)^T$
where k denotes the time instant and Δt the sample time.

In the remainder of the paper, the dynamic model (6) is compactly rewritten as:

$$x(k+1) = f(x(k), u(k)) \tag{7}$$

This paper focuses on a nominal control design, i.e. we assume perfect model knowledge (7) at the design stage and use feedback to correct for noise and model mismatch. Robust predictive control is subject of ongoing research.

III. Design of the Virtual Coupling MPC

A. Problem Description

We consider a convoy formed by n trains, as shown in Fig. 2.

In this convoy, each train is circulating at a velocity v^i at a distance $d^{i-1,i}$ of the preceding train.

For simplicity, we represent in Fig. 3 a convoy formed by two trains, composed by the leader and a follower, both of length L. The leader is circulating at a velocity v^l and the follower at v^f. The superscript denotes the train (l for the leader and f for the follower). The distance between train is calculated by means of (8).

$$d = s^l - s^f - L \tag{8}$$

The safety distance between trains d_{min} is used to define a hard constraint to avoid collision if the leader brakes in every driving conditions. If the train has a location error of $\pm e_s$ this distance is obtained with the expression (9):

$$d_{min} = d_0 + 2e_s \tag{9}$$

being d_0 the minimum required safe distance. This is a simple way of absorbing uncertainties in train location information. In our simulation, we have considered $e_s = \pm 0.5m$.

The distance d_{des} is used in the cost function as an objective to maintain a safer driving distance, greater than the minimum safe distance d_{min}.

We assume that the follower train has a sensor that allows to know the relative distance and relative velocity with the preceding train at any time. We also assume the presence of a communication link between both trains. This allows for the exchange of train state including position, velocity and acceleration.

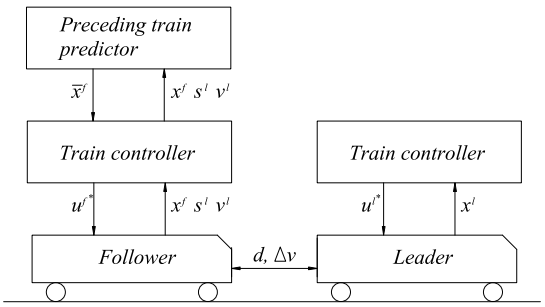

Fig. 4. Control architecture for the non-cooperative virtual coupling.

We consider that the convoy preserves its integrity, working as a unique train, when both trains arrive and stop at the same time in the same station with a minimum time delay between them.

B. Control Architecture for the Virtual Coupling

We consider a decentralized virtual coupling control with two different controllers, one for the front or *leader* and the other for the *followers* and we propose a Model Predictive Control (MPC) approach. Both controllers are nonlinear, and the constraints are explicitly handled [33].

According to the receding horizon principle, at each time step the MPC algorithm computes the optimal control and state trajectories solving a finite horizon optimization problem.

For the formulation of the MPC a prediction horizon $\left[t, t+N_p\right]$ is considered at time t. The notation $x_{t+k|t}$ represents the state vector at time $t+k$, predicted at time t, obtained by starting from the current state $x_{t|t} = x(t) \equiv x_t$, and where $u_{\cdot|t} = \left[u_{t|t}, \ldots, u_{t+N_p-1|t}\right]$ denotes the unknown input variables to be optimized.

We also use a Dynamic Programming (DP) approach [31] to precompute the reference behavior of the vehicle under control. The result of the DP establishes the general policy followed by the train convoy. This general control policy can have different objective functions like minimizing the energy consumption or maximizing the convoy speed. In this paper we have chosen the second policy with an optimal speed profile that finds the maximum velocity permitted by the speed limitations imposed by the line operation, i.e. satisfying the speed constraint at all time, maintaining a desired distance d_{des}, while satisfying a safety limit d_{min}.

The control architecture for the virtual coupling control is represented in Fig. 4. Because we are considering a decentralized virtual coupling control, the first train drives ignoring the presence of a follower, and its longitudinal dynamics follows the objective of the control for the leader, i.e. to move the train as fast as possible while satisfying the state and input constraints, since it is not interrupted by other trains from the front.

For the follower, we adopt an Adaptive Cruise Control design based on [35] which provides non-collision guarantees for a vehicle platoon. The main difference is that our railway

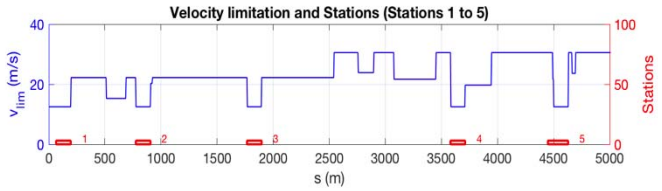

Fig. 5. Velocity limitation $v_{lim}(s)$ for the first five stations.

system is subject to a space-dependent velocity limit unlike a constant velocity limit in a vehicle platoon case.

For the follower, it is necessary a prediction of the preceding vehicle states $\bar{x}^f_{\cdot|t}$. In this case, the train controller uses a locally computed forecast about the preceding train states from its preceding train predictor, as can be seen in Fig. 4.

In the case of a multiple trains convoy, the block corresponding to the follower will be repeated for each following train.

C. Dynamic Programming for the Trains

A Dynamic Programming approach [31] has been used to precompute the optimal speed profile for each train.

For both trains, leader and follower, we precompute optimal speed profiles using DP with the goal of traveling at the fastest allowed speed while satisfying speed constraints at any time.

The speed constraint is shown in Fig. 5. For simplicity, just the first five stations have been included. The different stations are represented in the horizontal axis. This speed limitation is established by the design of the line, representing the maximum allowed speed v_{lim} depending on the position s of the train on the track.

This velocity profile is used as a constraint by the control system to guarantee that the train obey the speed limit restrictions at all times.

In this approach, the desired speed profile is specified as a function of space (i.e. position on the track) and a parametrization in space is used so that the independent variable is position s. This allows a considerable reduction in complexity for long tracks and also a space depended grid. The track is sampled with Δs so that s_i is the position of the train at step i, v_i the speed at position s_i, $S = [s_0, \ldots, s_{N_s}]$ is the discretized track and N_s is the number of discretization points.

Because of inertia, the train will not be allowed to travel at maximum speed at all time and the maximum speed is both a target and a constraint.

For each train, the optimization problem can be formulated as:

$$J^*_{i\to N_s}(v_i) = \min_u q(v_i, u_i) + J^*_{i+1\to N_s}(v_{i+1}) \tag{10a}$$

where:

$$q(v_i, u_i) = \|v_i - v_{lim}(s_i)\|_{K_{V_{DP}}} + \|(v_i - v_{lim}(s_i)) + |v_i - v_{lim}(s_i)|\|_{K_{L_{DP}}} \tag{10b}$$

subject to:

$$v_{i+1} = \sqrt{v_i^2 + 2\Delta s\left(-A - Bv_i - Cv_i^2 - F_g - u_i\right)/M} \tag{10c}$$

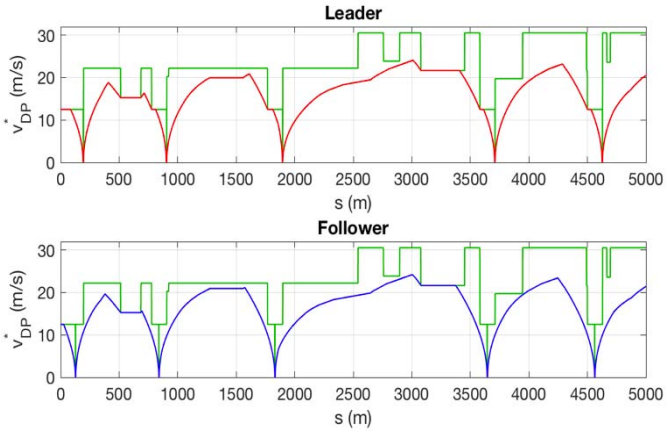

Fig. 6. Speed profile v^*_{DP} for the leader and follower (first 5 stations).

$$-Ma_{br} \le u_i \le Ma_{dr} \tag{10d}$$

$$-P_{br} \le v_i \cdot u_i \le P_{dr} \tag{10e}$$

$$0 \le v_i \le v_{lim}(s_i) \quad \forall i = N_s - 1, \ldots, 1 \tag{10f}$$

$$v_{N_s} = v_f \tag{10g}$$

$$J^*_{N_s\to N_s}(v_{N_s}) = \begin{cases} 0 & if\ v_N \le v_{lim}\left(s_{N_s}\right) \\ \infty & otherwise \end{cases} \tag{10h}$$

The different terms in the cost function (10a-b) have the following meaning: $K_{V_{DP}} \ge 0$ represents the weight penalizing the output deviation from the maximum allowed speed, and $K_{L_{DP}} \ge 0$ represents the weight penalizing overshooting the maximum allowed speed.

The equation (10c) is the space discretization model of (1) using a trapezoidal formula. Expressions (10d-e) represent the inputs constraints in force and power. Equation (10g) is the terminal constraint and (10h) represents the initial condition for the cost function (10a). Part of the solution of (10) represents the varying velocity trajectory due to the stops in each station and varying railroad characteristics and it is denoted as $v^*_{DP}(s)$.

For the DP we consider a variable Δs with a minimum of $\Delta s_{min} = e_s/2$, i.e. lower than the location error, and a maximum $\Delta s_{max} = 5$m. This minimum value is considered in the areas near to the stops in stations, where the distance between trains are shorter, being increased when the trains are circulating at a higher velocity and the distance between trains is higher. The right choice of Δs is important since in the DP computation grows quadratically with the number of sampling points.

Fig. 6 shows the speed profile $v^*_{DP}(s)$ obtained by solving (10) for the leader and the follower. The velocity $v^*_{DP}(s)$, which is computed offline, is used in the following control designs to guarantee that the train obeys the speed limit at all times.

D. Optimal Control Design

A Model Predictive Control (MPC) approach is proposed for the real time control of the trains. According to the receding horizon principle, at each time step the MPC algorithm

computes the optimal control and state trajectories solving a finite horizon optimization problem.

For the formulation of the MPC a prediction horizon $[t, t+N_p]$ is considered at time t. The notation $x_{t+k|t}$ represents the state vector at time $t+k$, predicted at time t, obtained by starting from the current state $x_{t|t} = x(t) \equiv x_t$, and $u_{\cdot|t} = [u_{t|t}, \ldots, u_{t+N_p-1|t}]$ denotes the unknown input variables to be optimized.

1) Optimal Control Design for the Leader: The objective of the control for the leader is to move the train as fast as possible while satisfying the state and input constraints. Therefore, the optimization problem can be formulated as:

$$\min_{u_{\cdot|t}} J = \sum_{k=t}^{t+N_p} K_V^l \cdot \left\| 1 - v_{k|t}^l / v_{max} \right\| \tag{11a}$$

$$+ \sum_{k=t}^{t+N_p-1} K_J^l \cdot \left\| j_{k|t}^l / j_{max} \right\| \tag{11b}$$

subject to:

$$x_{k+1|t}^l = f(x_{k|t}^l, u_{k|t}^l) \tag{11c}$$

$$x_{t|t}^l = x_t^l \tag{11d}$$

$$0 \le v_{k|t}^l \le v_{lim}(s_{k|t}^l) \tag{11e}$$

$$-j_{max} \le j_{k|t}^l \le j_{max} \tag{11f}$$

$$-Ma_{br}^l \le u_{k|t}^l \le Ma_{dr}^l \tag{11g}$$

$$-P_{br}^l \le v_{k|t}^l \cdot u_{k|t}^l \le P_{dr}^l \tag{11h}$$

$$\forall k = t, \ldots, t+N_p-1$$

$$0 \le v_{t+N_p|t}^l \le v_{DP}^{l*}\left(s_{t+N_p|t}^l\right) \tag{11i}$$

where:

$$j_{l_{k|t}} = (F_{k+1|t}^l - F_{k|t}^l) M / \Delta t \tag{11j}$$

The cost function (11a-b) has several dimensionless coefficients: $K_V^l \ge 0$ represents the weight penalizing the output deviation from the maximum allowed speed, and $K_J^l \ge 0$ represents the weight penalizing the input jerk.

Equations (11c) represents the system dynamics updates for the discrete-time model obtained from (7) applied to the leader. The initial state is set in (11h).

Equation (11d) corresponds to the velocity constraint v_{lim} as shown in Fig. 5. This is considered as a hard constraint because in real applications, exceeding the maximum speed is considered dangerous and automatically trigger the Automatic Train Protection system.

Equation (11e) represents the limitation of jerk defined in (11j) and obtained from state F^l. The input constraints (11f-g) include the limitation of maximum driving and braking force and the power limitation in driving and braking.

Equation (11i) represents a terminal constraint. The upper bound on the velocity $v_{DP}^{l*}(s)$ is obtained from the solution of the DP optimization problem (10). This terminal constraint is used because the train must obey the speed limit for all times and some states allowed by the track speed limit (upper red area in Fig. 7) may result in violation of the speed limit in the future times. By limiting the train velocity below v_{DP}^{l*} at its terminal time step, the train is guaranteed to have a feasible velocity trajectory which persistently obeys the velocity limit.

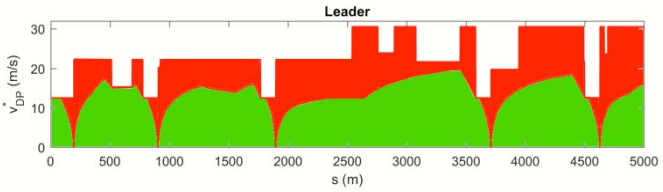

Fig. 7. Terminal set (only the first 5 stations are represented).

2) Optimal Control Design for the Followers: The objective of the follower control is to maintain a distance between the trains $d_{k|t}$ as close as possible to a desired spacing policy d_{des} in safe conditions, tracking the speed of the leader, and minimizing the jerk $j_{k|t}^f$. The superscript f denotes the follower.

The notation of $\bar{s}_k^l$ and $\bar{v}_k^l$ represents the predicted leader position and velocity at time k, respectively.

Therefore, the optimization problem for the follower can be formulated as:

$$\min_{u_{\cdot|t}} J = \sum_{k=t}^{t+N_p} K_D \cdot \left\| 1 - d_{k|t} / d_{des} \right\| \tag{12a}$$

$$+ \sum_{k=t}^{t+N_p} K_V^f \cdot \left\| \left(\bar{v}_{k|t}^l - v_{k|t}^f\right) / v_{max} \right\| \tag{12b}$$

$$+ \sum_{k=t}^{t+N_p-1} K_J^f \cdot \left\| j_{k|t}^f / j_{max} \right\| \tag{12c}$$

subject to:

$$x_{k+1|t}^f = f(x_{k|t}^f, u_{k|t}^f) \tag{12d}$$

$$x_{t|t}^f = x_t^f \tag{12e}$$

$$d_{min} \le d_{k|t} \tag{12f}$$

$$0 \le v_{k|t}^f \le v_{lim}(s_{k|t}^f) \tag{12g}$$

$$-j_{max} \le j_{k|t}^f \le j_{max} \tag{12h}$$

$$-Ma_{br}^f \le u_{k|t}^f \le Ma_{dr}^f \tag{12i}$$

$$-P_{br}^f \le v_{k|t}^f \cdot u_{k|t}^f \le P_{dr}^f \tag{12j}$$

$$\forall k = t, \ldots, t+N_p-1$$

$$0 \le v_{t+N_p|t}^f \le v_{DP}^{f*}\left(s_{t+N_p|t}^f\right) \tag{12k}$$

$$d_{min} \le d_{t+N_p|t} \tag{12l}$$

$$d_{min} \le d_{t+N_p|t} + \left(\bar{v}_{t+N_p|t}^l\right)^2 / 2a^l - \left(v_{t+N_p|t}^f\right)^2 / 2a^f \tag{12m}$$

where:

$$d_{k|t} = \bar{s}_{k|t}^l - s_{k|t}^f - L \tag{12n}$$

$$j_{k|t}^f = (F_{k+1|t}^f - F_{k|t}^f) M / \Delta t \tag{12o}$$

The cost function (12a-c) has several dimensionless coefficients: $K_D \ge 0$ is a dimensionless coefficient that represents the weight penalizing the output deviation from the desired distance and $K_V^f \ge 0$ is a dimensionless coefficient that represents the weight penalizing the deviation from the predicted preceding vehicle velocity. The term (12c) in the cost function has a similar meaning that for the leader. The terms (12a) and (12b) are specific for the follower.

The different constraints have also similar meaning that for the leader. Additionally to the constraints defined for

the leader, in the follower constraints, equation (12e) represents the safety condition stablishing that the distance between trains must be greater than d_{min} at any time.

Equations (12k-m) are the terminal constraints. They are imposed to guarantee that the controller is recursively feasible and safe. This can be guaranteed by constructing the terminal set as an invariant set [36]. To appropriately design the terminal set, we followed the work of [35]. Assuming the train dynamic model (7) as a simple kinematic point mass model capable of maximum deceleration a^f, and formulated as the set defined by (12k-m). It guarantees that the following vehicle can come to a full stop without collision when the leading train performs emergency braking with the maximum deceleration a^l. For more details on proving that the set defined by (12k-m) is an invariant set, we refer to the work in [35].

E. Closing the Loop

For each train, the resulting optimal states and inputs of (11-12) are denoted as following:

$$x_t^{i^*} = \begin{pmatrix} x_{t|t}^{i^*} & x_{t+1|t}^{i^*} & \dots & x_{t+N_p|t}^{i^*} \end{pmatrix}^T$$
$$u_t^{i^*} = \begin{pmatrix} u_{t|t}^{i^*} & u_{t+1|t}^{i^*} & \dots & u_{t+N_p-1|t}^{i^*} \end{pmatrix}^T \tag{13}$$

with $i = (l, f)$

It is noted that constraints (11c), (11d) and (11i) are space dependent. In order to prevent numerical issues and lessen the computational load, they can be a-priori estimated through $\overline{s}_{t+k|t}^i$, where:

$$\overline{x}_{k+1|t}^i = f(\overline{x}_{k|t}^i, \overline{u}_{k|t}^i) \quad \forall k = t, \dots, t+N_p-1 \tag{14a}$$
$$\overline{u}_{k|t}^i = u_{k|t-1}^{i^*} \quad \forall k = t, \dots, t+N_p-2 \tag{14b}$$
$$\overline{u}_{t+N_p-1|t}^i = u_{t+N_p-2|t-1}^{i^*} \tag{14c}$$
$$\overline{x}_{t|t}^i = x_{t|t}^i \tag{14d}$$

where $u_{k|t-1}^{i^*}$ is the input predicted from (13) at the previous time step *t-1* with $u_{k|-1}^{i^*} = 0 \forall k = 0, \dots, N_p - 2$.

For closing the loop, the first input is applied to the system (7) during the time interval $[t, t+1)$

$$u_t^i = u_{t|t}^{i^*} \tag{15}$$

At the next time step *t+1*, a new optimal problem in the form of (11-12), based on new measurement of the state, is solved over a shifted horizon, yielding a moving receding horizon control strategy with control law.

F. Preceding Train Predictor

Three different scenarios have been considered in order to show the differences and advantages of virtual coupling versus a moving block system. The difference between scenarios is the prediction for the leader.

In the first scenario we consider the case in which both vehicles are instrumented with a communication module. If the inter-vehicular communication is available, the prediction task is executed by the preceding vehicle and the predicted trajectory is communicated to the following one. In this case the follower knows at each time the position, velocity and acceleration predictions of the leader. Furthermore, the distance between them is measured by a sensor. In this case, called *short horizon* (SH), the MPC assumes that the information of the leader can be predicted in a short horizon N_p. Thus, the corresponding expressions for the predicted $\bar{s}_{k|t}^l$ and $\bar{v}_{k|t}^l$ are:

$$\bar{x}_{t|t}^l = \begin{pmatrix} s_{t|t}^l & v_{t|t}^l & F_{t|t-1}^{l^*} \end{pmatrix} \tag{16a}$$
$$\bar{x}_{k+1|t}^l = f(\bar{x}_{k|t}^l, \bar{u}_{k|t}^l) \quad \forall k = t+1, \dots, t+N_p-1 \tag{16b}$$

where:

$$\bar{u}_{k|t}^l = u_{k|t-1}^{l^*} \quad \forall k = t, \dots, t+N_p-2 \tag{16c}$$
$$\bar{u}_{t+N_p-1|t}^l = u_{t+N_p-2|t-1}^{l^*} \tag{16d}$$

being respectively $\bar{s}_{t|t}^l$ and $\bar{v}_{t|t}^l$ the measured position and velocity of the leader at t, $F_{t|t-1}^{l^*}$ the force at time t predicted from (13) at the previous time step *t-1* initialized with $F_{0|-1}^{l^*} = 0$, and $u_{k|t-1}^{l^*}$ the input predicted from (13) at the previous time step *t-1* with $u_{k|-1}^{l^*} = 0 \ \forall k = 0, \dots, N_p - 2$.

The second scenario, called *no prediction* (NP), corresponds to a degraded situation where the follower loses the communication link; therefore, the follower does not know the position, velocity, and acceleration predictions of the leader. If the inter-vehicular communication is not available, the prediction of the leader is carried by the follower. This prediction should be based on the information collected by onboard sensors, like the vehicle distance and its relative speed. In real operation, this case can only be applied if the communication is lost in a short period of time, because if not, the following train must brake to ensure a safety operation.

In this situation, the MPC measures the first states in the first point of the prediction horizon for the leader as its actual states, and for the rest of the prediction horizon, the preceding train is assumed to apply the worst conditions with maximum service braking. Thus, the corresponding expressions for the prediction of $\bar{s}_{k|t}^l$ and $\bar{v}_{k|t}^l$ result as:

$$\begin{cases} \bar{s}_{t|t}^l = s_{t|t}^l \\ \bar{v}_{t|t}^l = v_{t|t}^l \end{cases} \tag{17a}$$
$$\begin{cases} \bar{s}_{k|t}^l = \bar{s}_{k-1|t}^l + \bar{v}_{k-1|t}^l \Delta t - 0.5 a^l \Delta t^2 \\ \bar{v}_{k|t}^l = \max\left(\bar{v}_{k-1|t}^l - a^l \Delta t, 0\right) \end{cases} \quad \forall k = t+1, \dots, t+N_p \tag{17b}$$

being a^l the maximum service braking acceleration for the front train.

And the third scenario corresponds to the moving block (MB) train control system. This system considers the assumption that the follower must be separated by a sufficient margin to ensure every train is capable of braking and stopping before reaching the last known position of the leader.

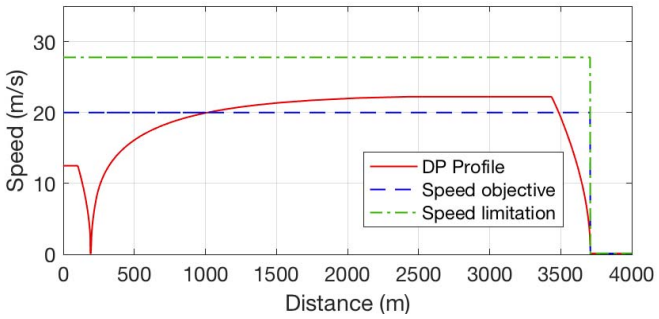

Fig. 8. Speed profile for the test environment.

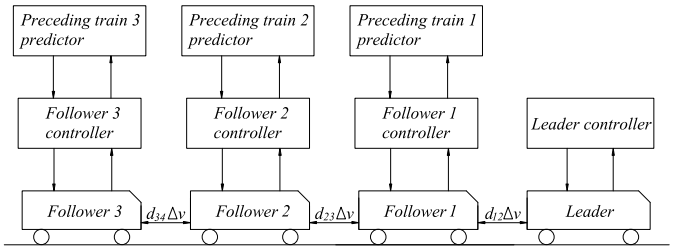

Fig. 9. Control scheme for a 4-trains convoy.

In this case the MPC assumes that the position for the leader remains as the current measured position $s^l_{t|t}$ and the leader velocity equals to zero at any point of the prediction horizon.

$$\begin{cases} \bar{s}^l_{k|t} = s^l_{t|t} \\ \bar{v}^l_{k|t} = 0 \end{cases} \quad \forall k = t, \ldots, t + N_p \tag{18}$$

IV. Simulations

A. Test Environment

Firstly, a basic scenario is developed to check and evaluate several basic aspects. This scenario is used to evaluate the influence of the horizon prediction length, the system performance when we use a convoy with multiple trains, and the differences between the three different prediction strategies.

The scenario consist of a simple maneuver of full acceleration until an objective speed of 20 m/s and a full emergency braking, stopping the convoy leader at a distance of 3.700 m from the origin.

Fig. 8 shows the speed line limitation of 27,78m/s, the maximum achievable speed profile of 23 m/s obtained from DP and the objective speed of 20m/s.

1) Multiple Trains Convoys Analysis: We consider a general convoy formed by n trains. In this convoy, the leader is controlled by (11) and each follower is controlled by (12). The preceding train predictions are obtained from (16). This scheme is shown in Fig. 9.

As we have considered a decentralized virtual coupling control architecture only is necessary to compute the controllers for each individual train, so the problem complexity increases linearly with the number of trains. Table I presents the computation time corresponding to different convoy lengths. In this table we can see how the computation time increases linearly.

Fig. 10 shows the velocity and distance between consecutive trains obtained for a four trains convoy.

TABLE I
Computation Time Obtained for Different Length of Trains Convoy

Num. trains	2	4	6	8
Comp. time (s)	709	1370	2117	2898

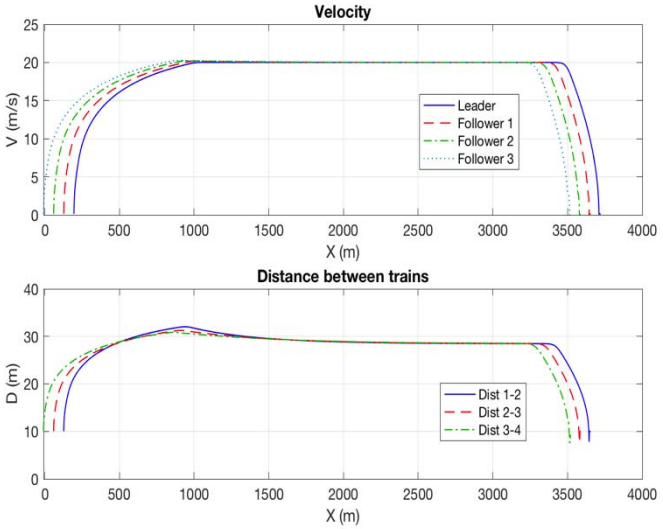

Fig. 10. Velocity and distance between consecutive trains obtained for a four trains convoy for the SH prediction strategy.

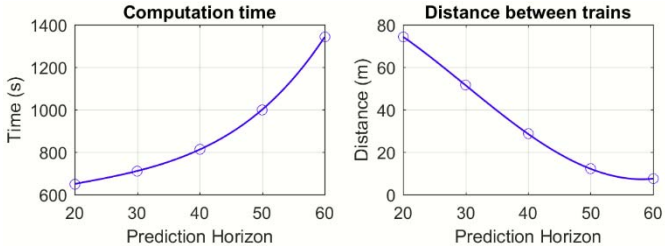

Fig. 11. Influence of the length of the prediction horizon.

2) Influence of the Length of the Prediction Horizon: Several simulations have also been run in order to select the most suitable prediction horizon in our simulations. With this aim, we have considered a two trains convoy and we have run several test with different predictions horizons, considering from 20 to 60. As expected, the computation time increases when the horizon prediction increases. But another interesting effect is that, for virtual coupling short horizon prediction, the distance between trains decreases when the prediction horizon increases. These results are shown in Fig. 11.

Based on these results, we have chosen a $N_p = 40$ because it produced a reasonable computation time and a shorter distance between trains than with shorter prediction horizons.

3) Differences Between Different Prediction Strategies: The last analysis done using the test environment is the comparison between the three considered prediction strategies (SH, NP and MB). We have also considered a two trains convoy and we have applied the three different predictions. Fig. 12 presents these results.

In Fig. 12, we can see how, for the test conditions, the distance between trains is much shorter for the short horizon prediction (28.5m) than for the moving block prediction (352.4m), obtaining an intermediate value between them

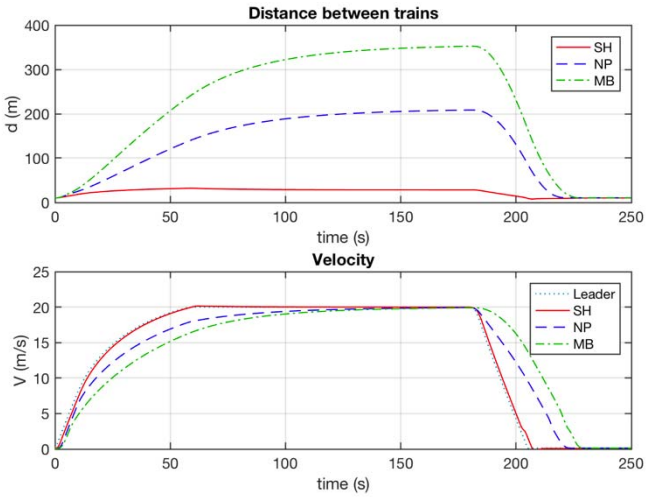

Fig. 12. Influence of the length of the prediction horizon.

for the NP (208.3m). And in the velocity plot, we can see how with the SH strategy used for virtual coupling, the follower tracks the leader speed and has no significant delay (only 2s), but for the NP and MB cases, the follower stops with important delay of 17s and 23s respectively, considering that in these cases the control does not preserve the convoy integrity.

B. Real Line Simulation Environment

As a second step, a real metro line simulation has been analyzed. The railway line considered corresponds to the Line 1 of Metro of Ho Chi Minh in Vietnam [30]. The parameters for the trains are included in Appendix.

In these simulations, we define the train convoy as a set of virtually coupled trains equivalent to a set of mechanically coupled trains, i.e. all the components of the train convoy must stop at the same time in a station. In our case the train convoy is formed by two trains. This is the basic configuration because the platform length limits the number of trains (the trains have a length approximately half of the platform size and the stopping points are at the end of the station for the leader and at the middle point for the follower).

The simulations only consider a single line and no crossing between different lines and switches have been analyzed.

The goal of this choice is to cover different situations in a single railway line with a basic convoy comparing distance and delay between trains.

All the simulations start with an initial condition in which the leader is leaving the first station, and the follower is leaving its stopping point inside the station, placed at a distance d_{min} from the leader, so it is as close as possible to the leader. Both trains stop in each station during 30 s.

In the simulation, it is assumed that both the leader and the follower are working at the maximum driving / braking power.

Ideal conditions have been considered, i.e. we have not considered uncertainties in position, distance, line profile (slope and radius) and time delay in receiving positional information.

Several cases have been analyzed for each scenario, taking different values for a^f in the terminal constraint that guarantees that the following vehicle can come to a full stop without collision. In all of them, $a^l = 1.25m/s^2$, i.e., the leader applies emergency braking. And a^f is analyzed in rank of $a^f \in [0.5\ 1]m/s^2$. The upper limit $a^f = 1m/s^2$ corresponds to the maximum service braking deceleration and the lower bound $a^f = 0.5m/s^2$ corresponds to a service braking deceleration limited to 50%.

The upper bound is a realistic situation in which both trains are braking as much as possible in normal conditions (maximum service braking) and, for the leader, the emergency braking can be understood as absorbing uncertainties as for example a change of slopes in the track. The lower bound is a conservative situation limiting the service braking deceleration to 50% and where the braking distance for the follower is higher.

C. Results

Two groups of simulations have been developed. The first one analyzes, for a given controller configuration, the differences between the SH, NP and MB control strategies. The second one studies, for the SH strategy, the effect of considering different controller parameter settings.

The results corresponding to $a^f = 1m/s^2$ appear in Fig. 13. In this figure, we can see that the best results are obtained for the short prediction horizon, with significant improvements in relation with the moving block.

Fig. 13a shows the velocities for the leader and for the different follower' strategies. Fig. 13b presents the distance between leader and follower for the SH, NP and MB control strategies. Fig. 13c represents the control input for each train. And Fig. 13d shows the velocity versus position, showing the track limitations and the location of the stopping points at stations for both trains.

Fig. 13a and 13b show the differences of behavior between the three control strategies. It appears a clear distinctive behavior between short horizon and moving block strategies, demonstrating that the SH maintains a much shorter distance between trains (more than six times) as seen in Fig. 13b. Another interesting difference, shown in Fig 13a, is that in the case of the MB, because of the average speed is lower, the follower arrives significantly late to the stations with respect to the leader, disregarding the idea of a train convoy because trains are not in the station at the same time. This effect does not appear in the case of SH, where the follower arrives almost at the same time to the station, maintaining the convoy formation.

These two effects have as consequence that the distance between trains is shorter for the virtual coupling strategy, maintaining safe conditions, allowing then a significant increase the capacity of the line, while the MB strategy is not able to maintain the integrity of the convoy.

For the NP strategy, results are between SH and MB, but much closer to SH than MB. In this case, the distance between trains is higher (double than SH), but the strategy maintains a short delay similar to the case of SH.

The next set of simulations corresponds also to the same trip in which the trains stop at any station assuming in this case that $a^f = 0.5m/s^2$ and $a^l = 1.25m/s^2$. This is equivalent to the assumption that the braking capacity for the follower is limited to 50%. This is a much more conservative assumption

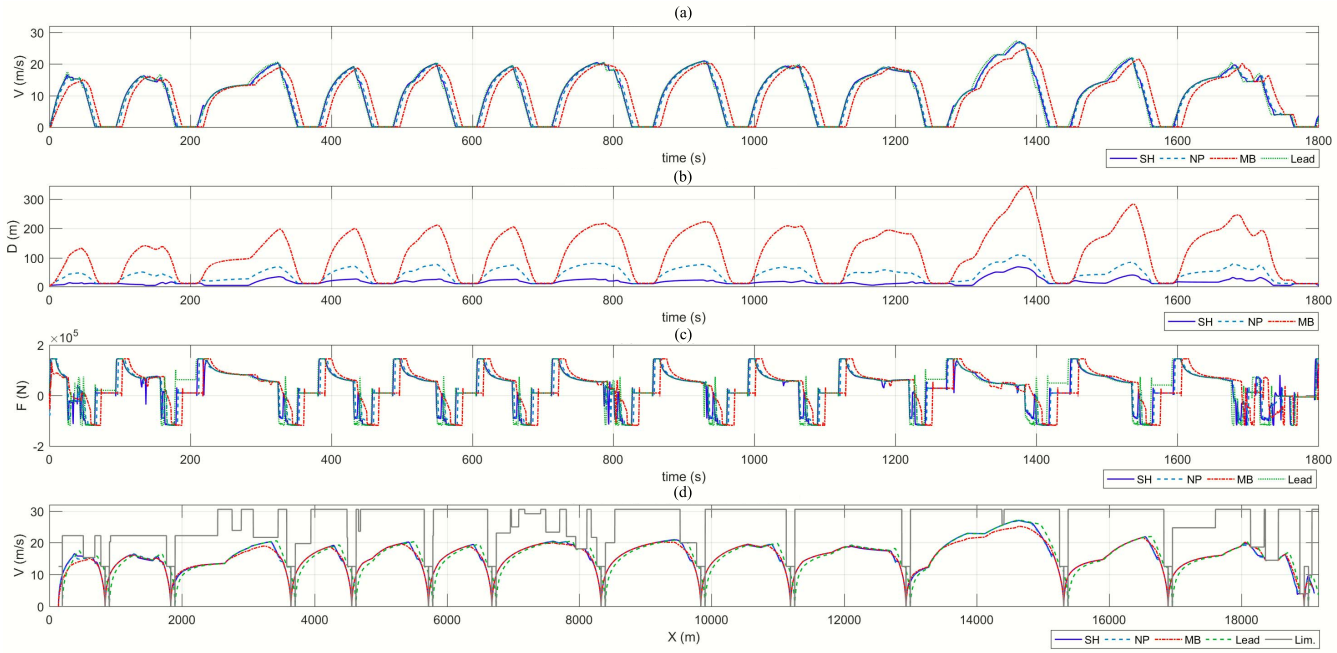

Fig. 13. Comparison between the different control strategies, with $a^f = 1m/s^2$. (a) Velocity vs. time. (b) Distance between trains vs. time. (c) Force (N) vs. time. (d) Velocity vs. position on the track.

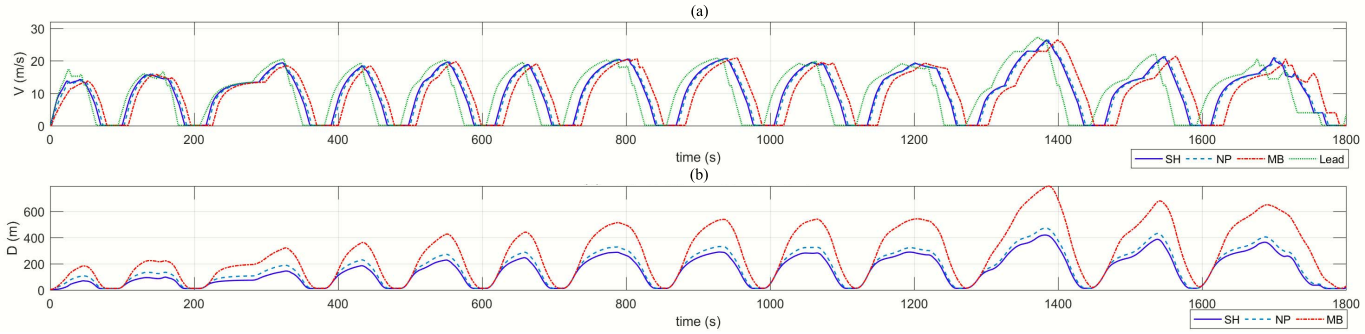

Fig. 14. Trains stop in each station and $a^f = 0.5m/s^2$. (a) Velocity vs. time. (b) Distance between trains vs. time.

in which the safe conditions imposed by the terminal constraint are significantly stricter.

The same three strategies have been simulated. Fig. 14 shows the obtained results. In this figure, we can see that again the best results are obtained for the short prediction horizon. Differences between SH and NP against MB are significant (more than two times in distance), but the most important difference is that the MB strategy is not able to maintain the convoy integrity in the stations, being the time delay between trains in the last part of the trip (stations 11 and higher) more than 30s, i.e. the trains are not able to stop at the same time in the same station.

Several intermediate cases have been also simulated, considering $a^f = 0.625\ m/s^2$, $0.75m/s^2$ and $0.875m/s^2$. Fig. 15 shows the summarized results. The results presented in this figure have been taken when the trains are entering to the 12^{th} station for the trains delay, and between station 12 and 13 in the point that presents the maximum distance between trains.

Fig. 15a shows the delay between trains when entering at station 12. This delay increases when the stations increase having the maximum value at this point. The results are

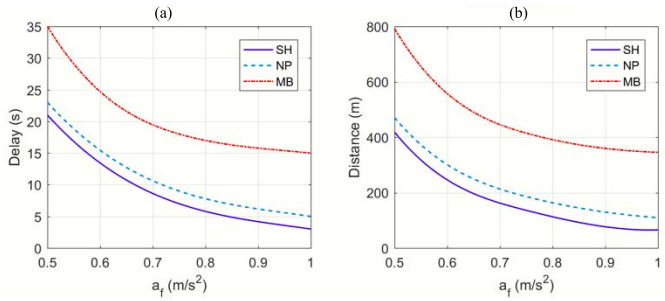

Fig. 15. Comparative plots between different control strategies and different a^f. (a) Delay. (b) Max. distance.

very interesting. It can be seen that the lower delays are obtained for the SH strategy, being slightly better than for NP. For SH, the delay is always below 30s, so the trains are in the station at the same time. In the case of $a^f = 1\ m/s^2$, the delay is very small (in fact, when $a^f > 0.8m/s^2$, $delay < 5$s). This means that, from an operational point of view, because of the delay is enough small, both trains are in the station at the same time and they can be considered as a unique train with double composition. But in the case of MB, the delay is higher

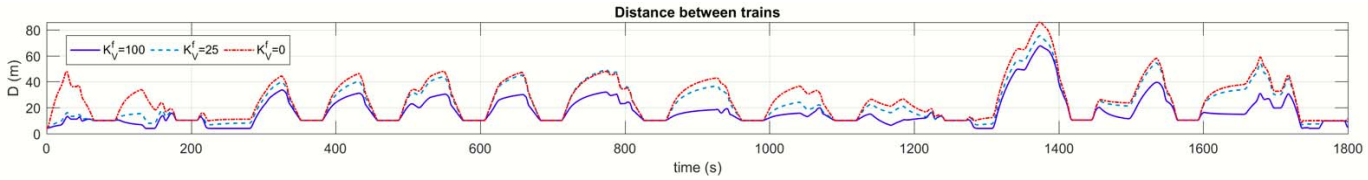

Fig. 16. Influence of the follower controller settings in the distance between trains.

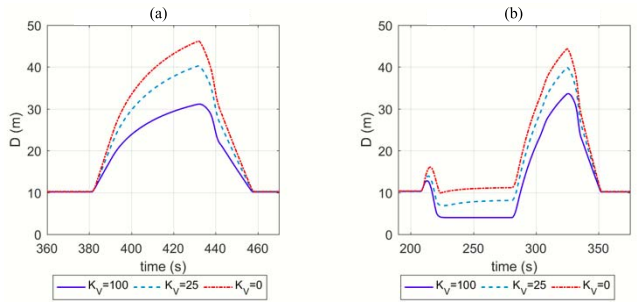

Fig. 17. Influence of the follower controller settings in the distance between trains. (a) Distance: Stations 4–5. (b) Distance: Stations 3–4.

(15s in the best case and 35s in the worst). These values mean that both trains are in the same station only a short time, and even they do not coincide at the same time in the station for the highest value of a^f.

The second set of simulations analyzes the effect of considering different settings for the follower's controller for the SH strategy. In the simulations $K_D = 100$ and $K_V^l = 100$, and three different values of K_V^f have been considered: 100, 25 and 0. The effect of varying K_V^f can be seen in Fig. 16.

The results show that the distance is higher when $K_V^f = 0$ than when $K_V^f = 100$. This means that, in the first case, the follower tries to circulate only at the desired distance d_{des} from the leader, but in the second case, the follower tries to circulate also at the maximum possible speed, reducing the distance between both trains. This produces a more aggressive behavior, as shown in more detail in Fig. 17.

Fig. 17a shows that when the track conditions are uniform, as occurs between stations 4 and 5 (Fig. 17a) the controller maintains the desired distance in stations and reduces the distance when K_V^f is applied. But when the track conditions vary, changing the slope, as happens between stations 3 and 4 (Fig. 17b), the controller with $K_V^f = 100$ is more aggressive prioritizing v in the cost function, reducing transitorily in this case the distance to the minimum safe distance.

V. Conclusions and Future Work

This paper has presented an innovative solution in the field of railways for the virtual coupling. This solution is originated on the ideas coming from the developments in the platooning of autonomous vehicles and is based on the model predictive control framework. Several control strategies have been developed and the results have been compared with the moving block train control concept. The results show significant behavior differences between the control strategies. The difference in behavior between short horizon and moving block strategies demonstrates that the MPC-based short prediction horizon strategy allows a much shorter distance between trains allowing then a significant increase in the capacity of the line. Another interesting difference for the moving block is that a significant retardation appears when the train arrives to the station, breaking the idea of being a train convoy. This effect does not appear in the case of SH, where the follower does not have delay, maintaining the convoy integrity. Therefore, results of the simulation demonstrate a better performance and benefits of this new concept versus the moving block system.

However, since this paper presents an initial approach based on a Nominal MPC, more evolved studies are necessary considering important issues as uncertainties in position, distance and line profile, or time delays that may appear in the reception of positional information. These aspects are subject of ongoing research.

TABLE II
Parameters

Model Parameters		MPC and DP Parameters	
Parameter	**Value**	**Parameter**	**Value**
$M\ (kg)$	1.608e+5	$\Delta t\ (s)$	0.1
$L\ (m)$	68	$d_{des}\ (m)$	10.0
$A\ (N)$	9155	$d_{min}\ (m)$	4.0
$B\ (Ns/m)$	633.6	$e_s\ (m)$	±0.5
$T_f C\ (Ns^2/m^2)$	46.84	N_p	40
τ	0.25	K_V^l	100
$P_{dr}\ (w)$	1.20e+06	K_J^l	0.5
$P_{br}\ (w)$	2.20e+06	K_D	{100, 25, 0}
$a_{dr}\ (m/s^2)$	0.9	K_V^f	100
$a_{br}\ (m/s^2)$	0.92	K_J^f	0.5
$j_{max}\ (m/s^3)$	0.98	$K_{V_{DP}}$	1.0
$a^l\ (m/s^2)$	1.25	$K_{L_{DP}}$	1.0e+05
$a^f\ (m/s^2)$	0.5 – 1.0	$\Delta s\ (m)$	0.25 - 5

Appendix

See Table II.

References

[1] *Standard for Communications-Based Train Control (CBTC) Performance and Functional Requirements*, IEEE Standard 1474.1-2004 (Revision of IEEE Standard 1474.1-1999), 2004. [Online]. Available: http://ieeexplore.ieee.org/stamp/stamp.jsp?tp=&arnumber=1405808&isnumber=30472. doi: 10.1109/IEEESTD.2004.95746.

[2] IRSE. (2017). *ERTMS Level 3: The Game-Charger*. [Online]. Available: http://www.irse.nl/resources/170314-ERTMS-L3-The-gamechanger-from-IRSE-News-Issue-232.pdf

[3] J. Beugin, C. Legrand, J. Marais, M. Berbineau, and E.-M. El-Koursi, "Safety appraisal of GNSS-based localization systems used in train spacing control," *IEEE Access*, vol. 6, pp. 9898–9916, 2018. doi: 10.1109/ACCESS.2018.2807127.

[4] H. Dong, S. Gao, and B. Ning, "Cooperative control synthesis and stability analysis of multiple trains under moving signaling systems," *IEEE Trans. Intell. Transp. Syst.*, vol. 17, no. 10, pp. 2730–2738, Oct. 2016. doi: 10.1109/TITS.2016.2518649.

[5] R. Liu, "Simulation model of speed control for the moving-block systems under ERTMS Level 3," in *Proc. IEEE Int. Conf. Intell. Rail Transp. (ICIRT)*, Aug. 2016, pp. 322–327.
[6] W. Sun, F. R. Yu, T. Tang, and S. You, "A cognitive control method for cost-efficient CBTC systems with smart grids," *IEEE Trans. Intell. Transp. Syst.*, vol. 18, no. 3, pp. 568–582, Mar. 2017. doi: 10.1109/TITS.2016.2586938.
[7] H. Wang, F. R. Yu, L. Zhu, T. Tang, and B. Ning, "A cognitive control approach to communication-based train control systems," *IEEE Trans. Intell. Transp. Syst.*, vol. 16, no. 4, pp. 1676–1689, Aug. 2015. doi: 10.1109/TITS.2014.2377115.
[8] J. Pochet, S. Baro, and G. Sandou, "Automatic train supervision for a CBTC suburban railway line using multiobjective optimization," in *Proc. IEEE 20th Int. Conf. Intell. Transp. Syst. (ITSC)*, Oct. 2017, pp. 1–6.
[9] B. Ning, J. Xun, S. Gao, and L. Zhang, "An integrated control model for headway regulation and energy saving in urban rail transit," *IEEE Trans. Intell. Transp. Syst.*, vol. 16, no. 3, pp. 1469–1478, Jun. 2015. doi: 10.1109/TITS.2014.2366495.
[10] L. Zhu, F. R. Yu, B. Ning, and T. Tang, "Design and performance enhancements in communication-based train control systems with coordinated multipoint transmission and reception," *IEEE Trans. Intell. Transp. Syst.*, vol. 15, no. 3, pp. 1258–1272, Jun. 2014. doi: 10.1109/TITS.2014.2298409.
[11] U. Bock and J. U. Varchmin, *Enhancement of the Occupancy of Railroads Using Virtually Coupled Train Formations*. Tokyo, Japan: World Congress on Railway Research, 1999.
[12] U. Bock and G. Bikker, "Design and development of a future freight train concept–'virtually coupled train formations,'" *IFAC Proc. Volumes*, vol. 33, no. 9, pp. 395–400, 2000.
[13] I. K. S. Braun and E. Schnieder, "Concepts on a future railway management system," in *Proc. 8th World Congr. Intell. Transp. Syst. ITS Amer., ITS Aust., ERTICO (Intell. Transp. Syst. Services-Eur.)*, 2001, pp. 1–8.
[14] S. Konig and E. Schnieder, "Modeling and simulation of an operation concept for future rail traffic," in *Proc. IEEE Intell. Transp. Syst. (ITSC)*, Aug. 2001, pp. 808–812.
[15] D.-I. T. Ständer, D.-I. J. Drewes, and D.-W.-I. I. Braun, "Operational and safety concepts for railway operation with virtual train-sets," *IFAC Proc. Volumes*, vol. 39, no. 12, pp. 261-266, 2006.
[16] C. Henke, M. Tichy, T. Schneider, J. Böcker, and W. Schäfer, "Organization and control of autonomous railway convoys," in *Proc. 9th Int. Symp. Adv. Vehicle Control*, Kobe, Japan, vol. 2, Oct. 2008, pp. 1–6.
[17] Shift2Rail. (2019). *The Rail Joint Undertaking*. [Online]. Available: http://www.shift2rail.org
[18] Shift2Rail. (Mar. 2015). *Shift2Rail Strategic Master Plan, Version 1.0*. [Online]. Available: http://ec.europa.eu/transport/modes/rail/doc/2015-03-31-decisionn4-2015-adoption-s2r-masterplan.pdf
[19] IRSE. (2016). *ERTMS Level 4, Train Convoys or Virtual Coupling*. [Online]. Available: http://www.irse.org/knowledge/publicdocuments/ITC%20Report%2039.pdf
[20] J. Goikoetxea, "Roadmap towards the wireless virtual coupling of trains," in *Proc. Int. Workshop Commun. Technol. Vehicles*. Cham, Switzerland: Springer, pp. 3–9, 2016.
[21] G. Mantovani and L. Ferrarini, "Temperature control of a commercial building with model predictive control techniques," *IEEE Trans. Ind. Electron.*, vol. 62, no. 4, pp. 2651–2660, Apr. 2015. doi: 10.1109/TIE.2014.2387095.
[22] J.-Q. Wang, S. E. Li, Y. Zheng, and X.-Y. Lu, "Longitudinal collision mitigation via coordinated braking of multiple vehicles using model predictive control," *Integr. Comput.-Aided Eng.*, vol. 22, no. 2, pp. 171–185, 2015.
[23] S. Di Cairano, H. E. Tseng, D. Bernardini, and A. Bemporad, "Vehicle yaw stability control by coordinated active front steering and differential braking in the tire sideslip angles domain," *IEEE Trans. Control Syst. Technol.*, vol. 21, no. 4, pp. 1236–1248, Jul. 2013. doi: 10.1109/TCST.2012.2198886.
[24] B. Zhu, H. Tazvinga, and X. Xia, "Switched model predictive control for energy dispatching of a photovoltaic-diesel-battery hybrid power system," *IEEE Trans. Control Syst. Technol.*, vol. 23, no. 3, pp. 1229–1236, May 2015. doi: 10.1109/TCST.2014.2361800.
[25] V. Turri, Y. Kim, J. Guanetti, K. H. Johansson, and F. Borrelli, "A model predictive controller for non-cooperative eco-platooning," in *Proc. Amer. Control Conf. (ACC)*, May 2017, pp. 2309–2314.
[26] Y. Zheng, S. E. Li, K. Li, F. Borrelli, and J. K. Hedrick, "Distributed model predictive control for heterogeneous vehicle platoons under unidirectional topologies," *IEEE Trans. Control Syst. Technol.*, vol. 25, no. 3, pp. 899–910, May 2017. doi: 10.1109/TCST.2016.2594588.
[27] J. Zhou and H. Peng, "Range policy of adaptive cruise control vehicles for improved flow stability and string stability," *IEEE Trans. Intell. Transp. Syst.*, vol. 6, no. 2, pp. 229–237, Jun. 2005.
[28] J. Guanetti, Y. Kim, and F. Borrelli, "Control of connected and automated vehicles: State of the art and future challenges," *Annu. Rev. Control*, vol. 45, pp. 18–40, May 2018.
[29] J. Zhang, F.-Y. Wang, K. Wang, W.-H. Lin, X. Xu, and C. Chen (2011), "Data-driven intelligent transportation systems: A survey," *IEEE Trans. Intell. Transp. Syst.*, vol. 12, no. 4, pp. 1624–1639, Dec. 2011. doi: 10.1109/TITS.2011.2158001.
[30] (2011). *Gonzalez R*. [Online]. Available: https://e-archivo.uc3m.es/handle/10016/12156
[31] S. Iwnicki, *Handbook of Railway Vehicle Dynamics*. Boca Raton, FL, USA: CRC Press, 2006.
[32] Q. Wu, M. Spiryagin, and C. Cole, "Longitudinal train dynamics: An overview," *Vehicle Syst. Dyn.*, vol. 54, no. 12, pp. 1688–1714, 2016.
[33] D. Q. Mayne, J. B. Rawlings, C. V. Rao, and P. O. Scokaert, "Constrained model predictive control: Stability and optimality," *Automatica*, vol. 36, no. 6, pp. 789–814, 2000.
[34] R. E. Bellman and S. E. Dreyfus, *Applied Dynamic Programming*. Princeton, NJ, USA: Princeton Univ. Press, 2015.
[35] V. Turri, *Look-Ahead Control for Fuel-Efficient and Safe Heavy-Duty Vehicle Platooning* (Doctoral dissertation, KTH Royal Institute of Technology), 2018.
[36] F. Borrelli, A. Bemporad, and M. Morari, *Predictive Control for Linear and Hybrid Systems*. Cambridge, U.K.: Cambridge Univ. Press, 2017.

Jesus Felez (M'97–SM'18) received the Mechanical Engineering and Ph.D. degrees from the University of Zaragoza, Spain, in 1985 and 1989, respectively.

He became a Full Professor with UPM, Spain, in 1997. He has served as a Thesis Advisor for 30 master's theses and eight doctoral dissertations. He has published over 70 technical papers and has been actively involved in over 30 Research and Development national and international projects with public competitive funding and more than 50 relevant Research and Development projects with private companies. He is an Expert in the field of railway technology, a member of the scientific commission for the railway sector in Spain, and the Head of the Research Group in Simulation in Mechanical Engineering, UPM. His research interests are in the areas of technologies applied to the future railways, in particular to train control systems.

Yeojun Kim received the B.S. degree in mechanical engineering from The University of Texas at Austin, Austin, TX, USA, in 2015. He is currently pursuing the Ph.D. degree in mechanical engineering with the University of California at Berkeley, Berkeley, CA, USA.

His current research interests include eco-friendly adaptive cruise control, the optimal control for the decentralized platoon systems, and the robust control and predictive control.

Francesco Borrelli (F'16) received the Ph.D. from the Automatic Control Laboratory, ETH-Zurich, Switzerland.

He was the Founder and the CTO of BrightBox Technologies Inc., a company focused on cloud-computing optimization for autonomous systems. He has been served as a Consultant for major international corporations since 2004. He is the Co-Director of the Hyundai Center of Excellence in Integrated Vehicle Safety Systems and Control, University of California at Berkeley (UC Berkeley), Berkeley, CA, USA. He is currently a Professor with the Department of Mechanical Engineering, UC Berkeley. He has authored over one hundred publications in the field of predictive control. He has authored the book *Predictive Control* (Cambridge University Press). His research interests are in the areas of model predictive control and its applications to automated driving and energy systems.